0273-2289/00/83/0095/$12.75

DNA Hydrolysis by Monoclonal Autoantibody BV 04-01

L. S. Rodkey,*[,1,6] G. Gololobov,[1] C. A. Rumbley,[2] J. Rumbley,[3] D. V. Schourov,[4] O. I. Makarevich,[4] A. G. Gabibov,[4] and E. W. Voss, Jr[5]

[1]Department of Pathology and Laboratory Medicine, University of Texas-Houston, Medical School, Houston, TX 77225-0708; [2]Department of Cell and Structural Biology, 505 South Goodwin Avenue, University of Illinois at Urbana-Champaign, Urbana, IL 61801 (Present Address: University of Pennsylvania School of Medicine, Department of Medicine, Allergy and Immunology Section, Philadelphia, PA 19104); [3]Department of Biochemistry, 600 South Matthews, University of Illinois at Urbana-Champaign, Urbana, IL 61801 (Present Address: University of Pennsylvania School of Medicine, Department of Biochemistry and Biophysics, Philadelphia, PA 19104); [4]Engelhardt Institute of Molecular Biology, Russian Academy of Sciences, Vavilova 32, Moscow 117984, Russia; [5]Department of Microbiology, 407 South Goodwin Avenue, University of Illinois at Urbana-Champaign, Urbana, IL 61801; [6]Department of Pathology and Laboratory Medicine, University of Texas-Houston, Medical School, P.O. Box 20708, Houston, TX 77225-0708

Abstract

Monoclonal anti-DNA autoantibody BV 04-01 catalyzed hydrolysis of DNA in the presence of Mg^{2+}. Catalysis was associated with BV 04-01 IgG, Fab, and single-chain-antibody (SCA) proteins. Cleavage of both ss and dsDNA was observed with efficient hydrolysis of the C-rich region of $A_7C_7ATATAGCGCGT_2$, as well as a preference for cleaving within CG-rich regions of dsDNA. Data on specificity of ssDNA hydrolysis and kinetic data obtained from wild-type SCA, and two SCA mutants were used to model the catalytically active antibody site using the previously resolved X-ray structure of BV 04-01. The resulting model suggested that the target phosphodiester bond is activated by induction of conformational strain. In addition, the antibody–DNA complex contained a Mg^{2+} coordination site composed of the L32Tyr and L27dHis side chains and a DNA 3′-phospho-

*Author to whom all correspondence and reprint requests should be addressed.

diester group. Induction of strain along with the metal coordination could be part of the mechanism by which this antibody catalyzes DNA hydrolysis. Sequence data for BV 04-01 V_H and V_L genes suggested that the proposed catalytic-antibody active site was germline-encoded. This observation suggests that catalytic activity might represent an important—rarely examined—function for some antibody molecules.

Index Entries: Catalysis; autoantibody; abzyme.

Introduction

The usual perception of the relationship between antigen–antibody interactions and enzyme–substrate interactions is summarized by the following quote from Kuby's textbook of immunology: "The antigen-antibody interaction is a bimolecular association similar to an enzyme-substrate interaction but with the important distinction that it does not lead to an irreversible chemical alteration in either the antibody or antigen and therefore is reversible" *(1)*. However, Jencks *(2)* suggested in 1969 that antibodies might be capable of cleaving antigen if antibodies specific for an activated complex were made. In 1986, the research groups of Schultz and Lerner demonstrated that antibodies elicited against tetrahedral, negatively-charged phosphate and phosphonate transition-state analogs could selectively catalyze the hydrolysis of carbonates and esters, respectively *(3,4)*. Since their original discovery, catalytic antibodies have been used as mechanistic models for enzyme reactions, and numerous reactions—ranging from amide-bond cleavage to carbon–carbon bond forming and breaking—have been shown to be catalyzed by antibodies *(5)*. Reports of catalytic antibodies elicited against ground-state molecules *(6)* and the report of acetylcholine hydrolysis by antiidiotypic antibodies specific for acetylcholine esterase antibodies *(7)* indicate that catalytic antibodies also may be elicited without the requirement for using transition-state analogs for immunization. Reports of catalysis by naturally occurring human autoantibodies *(8–10)* suggest that catalytic antibodies may have a functional role in some autoimmune diseases.

Herron et al. *(11)* resolved the X-ray crystal structure of the liganded Fab fragment of MAb BV 04-01. Examination of the crystal structure showed that optimal $(dT)_3$ accommodation in the active site included intercalation of the second thymine base into a hydrophobic pocket formed by TyrL32 and TrpH100a, with additional stabilization provided by hydrogen bonds with SerL91. In addition, the sugar–phosphate chain of the $(dT)_3$ ligand was bent by the insertion of the side chain of HisL27d between nucleotides two and three. These as well as other interactions caused the bound sugar–phosphate backbone to adopt a conformation different from the solution conformation. Since Gabibov and colleagues *(12)* had suggested that conformational strain introduced into the ground state of the phosphodiester bond could be the mechanism for DNA-hydrolyzing activity

of the naturally occurring DNA autoantibody they studied, we hypothesized that enzymatic studies of BV 04-01 might be worthwhile.

This article characterizes the DNA-hydrolyzing activity associated with BV 04-01 IgG, Fab, and single-chain-antibody (SCA) proteins, and describes the kinetics and specificity of DNA hydrolysis. In addition, a model of the catalytic antibody-active site based on the catalytic activity of wild-type and mutant SCA proteins and the known X-ray crystal structure of BV 04-01 is proposed. These studies are described in greater detail in ref. *13*.

Materials and Methods

All materials and methods are described in detail in ref. *13*. Summaries are provided here.

SCA BV 04-01—Wild-type SCA 04-01 and SCA 04-01 L32Phe were constructed as described by Rumbley et al. *(14)*. Single-chain Fv 04-01 L27dAla mutant was constructed as described in ref. *13*. Expression and refolding of wild-type and mutant SCA 04-01 was done according to Denzin et al. *(15)*.

Fab fragments—Fab fragments were prepared by papain digestion of affinity-purified BV 04-01 as described in ref. *14*.

Purification of BV 04-01 MAb, Fab 04-01, and SCA 04-01—BV 04-01 antibody, Fab 04-01, and refolded SCA 04-01 as well as SCA 04-01 mutants were purified by adsorption on ssDNA-agarose, eluted with PBS containing 1 *M* NaCl. Elutes were further purified by passage through a gel filtration column.

DNA-nicking activity assay—One microgram of plasmid DNA (pUC19) was incubated with test sample in Tris buffer containing 10 m*M* MgCl2 and 50 m*M* NaCl. The reaction was terminated by addition of SDS to a final concentration of 1%, as described by Shuster et al. *(9)*.

Oligonucleotide cleavage—5′ P^{32}-labeled oligonucleotides (dT)15, (dA)14, and oligonucleotide $A_7C_7ATATAGCGCGT_7$ were mixed with test sample at 37°C in Tris buffer, and cleavage products were separated with 20% denaturing PAGE.

Digestion of dsDNA fragments by DNAse I and wild-type SCA 04-01—The double-stranded 147-bp EcoR1-Bgl1 fragment of pUC19 was labeled on the 3′ end with P^{32} and incubated with test sample, and digestion products were analyzed on 20% denaturing PAGE.

Modeling of Mg^{2+}-bound 04-01 active site—Modeling of the 04-01 active site was done using the PC version of HyperChem release 3.0, using the liganded crystal structure of the BV 04-01 Fab fragment. The structure was exported into the RasMol graphics display program, version 2.4.

Apparent kinetic constants—Apparent kinetic constants were determined by sequential measurements of cleavage on agarose gels with ethidium bromide staining, as described in ref. *16*.

Table 1
Apparent Kinetic Constant Values for the Plasmid DNA Hydrolysis by SCA 04-01 Wild-Type and Mutants Calculated by Fitting Initial Values into the Michaelis–Menten–Henri Equation[a]

SCA Variant	K_m	k_{cat}	k_{cat}/K_m
L32Tyr/L27dHis (WT)	$(2.62 \pm 0.37) \times 10^{-8}$ *M*	$(1.61 \pm 0.07) \times 10^{-2}$ min^{-1}	6.15×10^5 M^{-1} min^{-1}
L32Phe/L27dHis	$(8.15 \pm 1.01) \times 10^{-9}$ *M*	$(1.73 \pm 0.05) \times 10^{-3}$ min^{-1}	2.12×10^5 M^{-1} min^{-1}
L32Tyr/L27dAla	$(2.25 \pm 0.21) \times 10^{-8}$ *M*	$(7.36 \pm 0.20) \times 10^{-4}$ min^{-1}	3.27×10^4 M^{-1} min^{-1}

[a]Values are means ± S.E.M. (From ref. *13*)

Results

Preliminary studies indicated that MAb 04-01, Fab 04-01, and SCA 04-01 derivatives could all introduce single-stranded breaks into supercoiled plasmid DNA in the presence of Mg^{2+} ions. The Fab fragment appeared to have greater catalytic activity than the intact IgG. This suggested that the presence of Fc had some inhibitory effect on catalysis.

Further studies using single-stranded oligonucleotides showed that both 5′-labeled homooligonucleotides (dT)15 and (dA)14 were hydrolyzed by SCA 04-01. SCA 04-01 hydrolyzed the (dT)15 preferentially at the 3′-end in an endonuclease-like manner. (dA)14 was also hydrolyzed by SCA 04-01 with approximately the same efficiency, but internal sequences were preferentially cleaved. Additional studies with a mixed sequence single-stranded oligonucleotide were also carried out. Cleavage-specificity studies using labeled single-stranded $A_7C_7ATATAGCGCGT_7$ revealed high specificity for cleavage of the C-rich region.

Other studies were initiated to study cleavage of dsDNA. The double-stranded 147 bp EcoR1-Bgl1 restriction fragment of pUC19 was treated with wild-type SCA 04-01, and with DNAse1 for comparison. The results showed that SCA 04-01 and DNAse1 had significantly different cleavage patterns. Major cleavage sites using SCA 04-01 were: 1) AGGˆGGG; 2) AGCˆGGA; 3) AATGˆGG; and 4) GGGˆACCG.

Wild-type SCA 04-01 (L32Tyr, H100aTrp) and two SCA 04-01 mutants (L32Phe and L27dAla) were used to investigate kinetic parameters of cleavage of supercoiled plasmid DNA. Since cleavable sites present in the plasmid were not equivalent (as was evident from studies of dsDNA fragment digestion), apparent catalytic constants were determined with the apparent k_{cat} representing the sum of individual k_{cat} [$k_{cat\ app} = (k_{cat\ 1} + \cdots + k_{cat\ n})$] and the apparent K_m representing the average of individual K_m [$K_{m\ app} = (K_{m\ 1} + \cdots + K_{m\ n})/n$]. Measurements of kinetic constants for both mutants were done using an excess of the optimal Mg^{2+} concentration that was previously determined for the wild-type SCA, and thus did not reflect the loss of antibody catalytic potency due to deterioration of Mg^{2+} affinity for the antibody–DNA complex. The data are presented in Table 1. Replacement

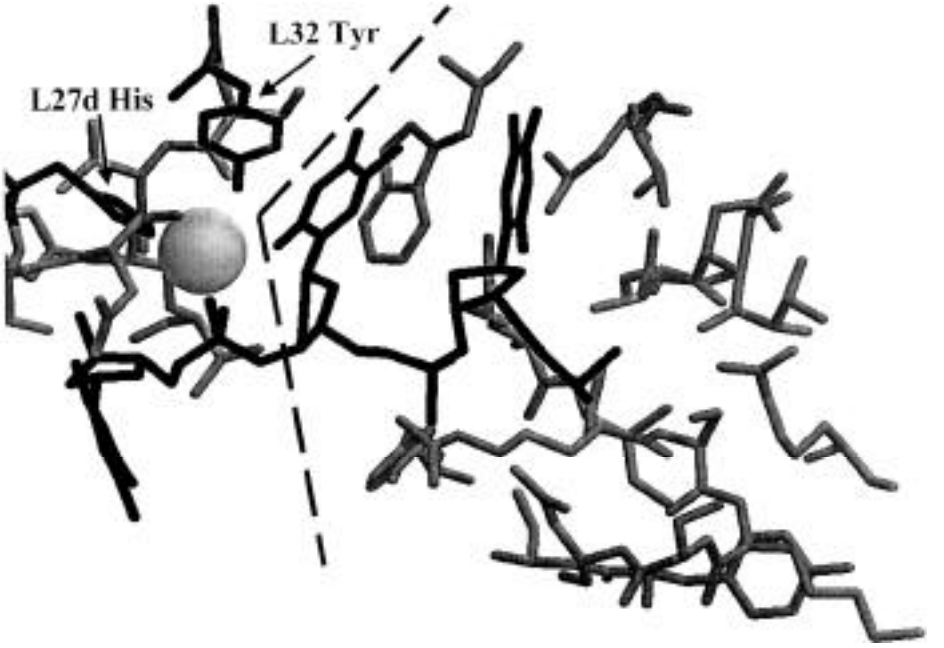

Fig. 1. Molecular model of Mg^{2+} ion accommodation by the BV 04-01 active site. The $(dT)_3$ ligand is shown in black, and all amino-acid residues within 7.5Å of the phosphates in $(dT)_3$ are shown in gray, except L27dHis and L32Tyr, which are gray with arrows. The Mg^{2+} ion is shown as a gray sphere. (From ref. *13*.)

of Tyr with Phe at position L32 resulted in a 10-fold decrease of k_{cat} with a simultaneous decrease (three-fold) in K_m. Replacement of L27dHis with Ala resulted in nearly unchanged K_m and a substantial reduction (22-fold) in k_{cat}. DNA hydrolysis by both mutants was nearly undetectable at Mg^{2+} concentration of 1 m*M*, while the wild-type SCA retained essentially all its catalytic efficiency (data not shown) under these conditions. Further measurements of reaction rates for DNA hydrolysis at different concentrations were made. The results showed *(13)* that the data fit the Michaelis–Menten–Henri equation, thus confirming the accuracy of the assay measurements.

The observation that the catalytic activity of 04-01 was significantly enhanced in the presence of Mg^{2+} leads to the question of how Mg^{2+} might be functioning to facilitate catalysis. To gain some insight into this question, we utilized the known crystallographic structure of BV 04-01 to construct a molecular model of the liganded site containing Mg^{2+}. The model is shown in Fig. 1. The Ig heavy-chain residues are to the right of the dashed line, and the light-chain residues are to the left. The Mg^{2+} ion is shown as a sphere. The darker (dT)3 ligand spans the light- and heavy-chain residues, and the light-chain L27dHis and L32Tyr are indicated and darkened in the model. The L32Tyr and L27dHis side chains and the 3′-phosphate group

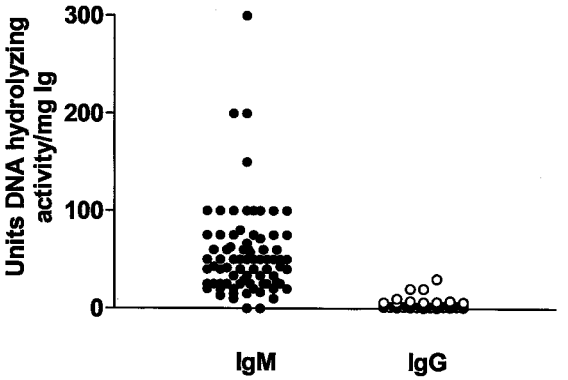

Fig. 2. Comparison of specific activities of IgM and IgG preparations isolated from the same serum. Catalysis of plasmid DNA by affinity-purified Ig was measured in arbitrary units where 1 unit of activity corresponded to complete relaxation of 0.2 μg DNA when incubated at 37C for 16 h. Specific activity was then calculated based on concentration of Ig in each sample. Each dot represents a separate sample.

of the (dT)3 ligand were aligned in order to stabilize Mg^{2+} coordination. Adequate space was available to accommodate the Mg^{2+} ion near the 3′-phosphodiester bond (grey sphere), and it appeared that additional conformational alteration was induced in the third phosphodiester bond in the ligand when Mg^{2+} was present. Importantly, no obvious changes were observed in the conformation of the amino-acid residues in the Mg^{2+} bound model when it was compared to the (dT)3 liganded X-ray structure.

Since the antibody BV 04-01 was originally isolated from an unmanipulated NZB/NZW F1 mouse that spontaneously develops anti-DNA antibodies and other lupus-like symptoms, studies of human lupus sera were conducted to determine whether the catalytic activity of IgM and IgG was equivalent. Affinity chromatography was used to isolate the total IgM fraction, and the total IgG fraction from each of 100 SLE sera was supplied by Dr. Frank Arnett from the University of Texas-Houston Medical School. Samples were mixed with 1 μg supercoiled plasmid, and the degree of cleavage of plasmid was measured in arbitrary units where 1 unit of activity corresponded to complete relaxation of 0.2 μg of plasmid DNA in 16 h. The value was then divided by the concentration of Ig (mg/mL) and expressed as total units DNA-hydrolyzing activity/mg Ig. Results, as shown in Fig. 2, showed that there was a significantly higher specific activity for IgM compared to IgG from the same sera. On average, there was an approximately 17× higher efficiency of cleavage for IgM vs IgG.

Discussion

Autoantibody BV 04-01 has been extensively characterized, including resolution of the X-ray crystal structure of the Fab fragment with bound (dT)3. The conformation of the $(dT)_3$ sugar–phosphate backbone in the

crystal structure was strained, and differed significantly from the backbone conformation that $(dT)_3$ would adopt in solution. The strain introduced in the phosphate backbone by the antibody active site suggested that BV 04-01 might possess catalytic activity.

Initial studies in our laboratory showed that BV 04-01, its Fab fragment, and the SCA 04-01 efficiently cleaved plasmid DNA in the presence of 10 m*M* Mg^{2+}. In addition, several mutant SCA proteins had catalytic activity. The source of catalytic activity correlated directly with the structural features of the antibodies and SCA proteins, and was not caused by the presence of contaminant nuclease. The BV 04-01 IgG was isolated from murine ascites fluid and purified by ammonium sulfate precipitation with subsequent affinity chromatography. The Fab fragments were prepared by papain digestion of affinity-purified whole BV 04-01 antibody and were then subjected to two additional affinity-chromatography purification steps. Wild-type and mutant SCA derivatives, on the other hand, were isolated from guanidine–HCl denatured *Escherichia coli*-derived inclusion bodies and refolded in vitro prior to an affinity chromatography step. Owing to the vastly different methods of protein expression (mammalian vs bacterial) and isolation, it cannot be convincingly argued that the observed similar catalytic activity of Fab and wild-type SCA 04-01 is due to a contaminating nuclease present in both murine and bacterial preparations, which is also found in equal concentrations following the papain digestion and affinity-purification protocol vs the in vitro denaturation and refolding protocol. Further, after affinity purification, all antibody proteins were purified by gel-filtration chromatography and HPLC. DNA-nicking activity was not detected in any HPLC elution fraction that did not correspond to the molecular weights of the IgG, Fab, or SCA proteins. Finally, it would be expected that if contaminating nucleases were responsible for the observed catalysis, all SCA proteins tested should possess similar catalytic activity. However, our results convincingly show that wild-type SCA and site-directed SCA mutants all possess *different* catalytic activities, including different k_{cat} and K_m values. Clearly, these data reflect differences in catalytic activity of the different BV 04-01 derivatives rather than contaminating nucleases.

Cleavage of ssDNA was not highly specific for any particular base sequence. Homooligonucleotide (dT)15 was cleaved preferentially on the 3′ side of the oligonucleotide, and the cleavage pattern for (dA)14 was different. A third oligonucleotide—$A_7C_7ATATAGCGCGT_7$—was also examined. Wild-type SCA 04-01 cleaved this substrate with the highest efficiency, and displayed strong specificity for the cleavage of the C-rich region.

The dsDNA 147-bp fragment was also hydrolyzed by SCA 04-01, and showed a far different cleavage pattern than that produced with DNAse1. The observed weak binding of BV 04-01 to dsDNA fragments *(17)* suggests that partial dsDNA unwinding may occur to allow formation of a productive cleavage complex with the antibody. Preference for cleavage of GC-rich regions was evident, although factors that govern specificity for

dsDNA substrate can be rather complex and can depend on the stability of the DNA duplex surrounding the cleavage site.

The SCA mutants, along with wild-type SCA04-01, were used to investigate kinetic parameters of the cleavage of supercoiled plasmid DNA. Reaction rates for DNA hydrolysis at different concentrations fitted the Michaelis–Menten–Henri equation, confirming the accuracy of the assay measurements. Both mutants showed a substantial reduction in their specific activities when measurements were done in substrate excess as compared to the wild-type SCA. As stated in the Results section, apparent kinetic constants (k_{cat} and K_m) determined with plasmid DNA as a substrate represent an additive value of the individual k_{cat} and average values of the individual K_m for each cleavage site on the substrate. Thus, changes in apparent kinetic constant values would reflect global changes in the antibody-catalytic machinery that are not dependent on a particular base sequence of the substrate. The 10-fold decrease of k_{cat} (*see* Table 1) and the simultaneous decrease of K_m (threefold) observed for the L32Phe mutant suggested that tighter plasmid–substrate binding contributed to the observed loss of specific activity for that mutant. The efficiency of DNA hydrolysis by this mutant (k_{cat}/K_m) was only three times less than the wild-type SCA. However, the effect of mutation on the catalytic rate was dramatic with respect to Mg^{2+} affinity for the antibody–DNA complex. Activity of the mutant was not seen at Mg^{2+} concentrations below 1 m*M*, while activity of the wild-type SCA was readily detectable. The L27dAla mutant possessed only 4.6% of the wild-type turnover rate, with nearly identical K_m. This 20-fold drop in efficiency compared to the wild-type SCA suggested that L27dHis was an important residue involved in catalysis. X-ray modeling of BV 04-01 showed that the L27dHis side chain caused bending of the ligand, presumably activating one of the phosphodiester bonds in the complexed oligonucleotide. The kinetic results observed with the L27dAla mutant suggested that DNA-substrate bending was contributing to the catalysis.

Sequence studies of BV 04-01 *(17)* revealed that in contrast to the heavy chain, the light-chain sequence is encoded by nearly unmutated VκII germline gene K5.1 *(18)*. This observation leads to the hypothesis that an antibody germline gene could encode DNA-hydrolyzing activity. The idea that antibodies could possess primordial catalytic activity was formulated by Greller and Erhan *(19)*, who observed a high degree of sequence homology between CDR1 of an antibody light chain and a fragment of the serine protease active site. Recently, several groups have reported proteolytic *(20)* and DNA-hydrolyzing *(21)* activities of antibodies and their subunits that are expression products of immature antibody genes. The results reported here, which show a higher DNA-catalytic specific activity for IgM vs IgG from the same serum, can be interpreted in several ways. One argument is that a higher fraction of the IgM molecules are catalytic, since the B-cell clones expressing IgM catalytic activity were present in larger numbers because they had not matured further, as compared with the IgG clones

expressed at that time. Another interpretation is that catalytic activity may have decreased during B-cell maturation to IgG synthesis because of the mutational loss of critical residues that contributed to catalytic activity. The data do not allow us to distinguish between these explanations. Further studies are necessary to clarify the significance of antibody-mediated catalytic activity in immune-system function.

Acknowledgments

Supported, in part, by an ISF grant to AGG and by a Procter and Gamble fellowship to CAR.

References

1. Kuby, J. (1992), *Immunology*. W. H. Freeman and Co., NY.
2. Jencks, W. P. (1969), *Catalysis in Chemistry and Enzymology*. McGraw-Hill, NY.
3. Pollack, S. J., Jacobs, J. W., and Shultz, P. G. (1986), *Science* **234,** 1570–1573.
4. Tramontano, A., Janda, K. D., and Lerner, R. A. (1986), *Science* **234,** 1566–1570.
5. Benkovic, S. J. (1992), *Ann. Rev. Biochem.* **61,** 29–54.
6. Paul, S., Sun, M., Mody, R., Tewary, H. K., Stemmer, P., Massey, R. J., Gianferrara, T., Mehrotra, S., Dreyer, T., Meldal, M., and Tramontano, A. (1992), *J. Biol. Chem.* **267,** 13142–13145.
7. Izadyar, L., Friboulet, A., Remy, M. H., Roseto, A., and Tomas, D. (1993), *Proc. Natl. Acad. Sci. USA* **90,** 8876–8880.
8. Paul, S., Volle, D. J., Beach, C. M., Johnson, D. R., Powell, M. J., and Massey, R. J. (1989), *Science* **244,** 1158–1162.
9. Shuster, A. M., Gololobov, G. V., Kvashuk, O. A., Bogomolova, A. E., Smirnov, I. V., and Gabibov, A. G. (1992), *Science* **256,** 665–667.
10. Li, L., Paul, S., Tyutyulkova, S., Kazatchkine, M. D., and Kaveri, S. (1995), *J. Immunol.* **154,** 3328–3332.
11. Herron, J. N., He, X. M., Ballard, D. W., Blier, P. R., Pace, P. E., Bothwell, A., Voss, E. W., Jr., and Edmundson, A. B. (1991), *Proteins Struct. Funct. Genet.* **11,** 159–175.
12. Gabibov, A. G., Gololobov, G. V., Makarevich, O. I., Schourov, D. V., Chernova, E. A., and Yadav, R. P. (1994), *Appl. Biochem. Biotechnol.* **47,** 293–303.
13. Gololobov, G. V., Rumbley, C. A., Rumbley, J. N., Schourov, D. V., Makarevich, O. I., Gabibov, A. G., Voss, E. W., and Rodkey, L. S. (1997), *Mol. Immunol.* **34,** 1083–1093.
14. Rumbley, C. A., Tetin, S. Y., Denzin, L. K., Yantz, L., and Voss, E. W., Jr. (1993), *J. Biol. Chem.* **268,** 13667–13674.
15. Denzin, L. K., Whitlow, M., and Voss, E. W., Jr. (1991), *J. Biol. Chem.* **266,** 14,095–14,103.
16. Gololobov, G. V., Chernova, E. A., Schourov, D. V., Smirnov, I. V., Kudelina, I. A., and Gabibov, A. G. (1995), *Proc. Natl. Acad. Sci. USA* **92,** 254–257.
17. Smith, R. G. and Voss, E. W., Jr. (1990), *Mol. Immunol.* **27,** 463–470.
18. Corbet, S., Milili, M., Fougereau, M., and Schiff, C. (1987), *J. Immunol.* **138,** 932–939.
19. Greller, L. D. and Erhan, S. (1974), *Int. J. Pept. Protein Res.* **6,** 165–173.
20. Matsuura, K., Yamamoto, K., and Sinohara, H. (1994), *Biochem. Biophys. Res. Commun.* **204,** 57–62.
21. Gololobov, G. V., Mikhalap, S. V., Starov, A. V., Kolosnikov, A. F., and Gabibov, A. G. (1994), *Appl. Biochem. Biotechnol.* **47,** 305–315.

Discussion

Schowen: Another possible role of the histidine is that it could remove a proton from a water molecule used to attack the phosphate linkage, or even to attack the phosphate linkage itself.

Rodkey: I think any comments related to those mechanisms are best answered by my coauthor, Dr. Gololobov.

Gololobov: Our proposed mechanism is based mainly on the X-ray structure. There is a histidine diad. We know that metals are important for catalysis, and that feature fits with the structural model.

Green: Scott, your presentation was very interesting. First, there is really no difference between the induced-fit model and transition-state stabilization as mechanisms of catalysis, because the latter includes all of the energetic effects required for catalysis. You described your work with IgM samples and IgG samples. The implication is that almost all of the antibodies that bind are catalytic. Then you described a particular monoclonal that expresses the catalytic activity. Were other monoclonal antibodies also catalytic? Second, in the control reactions without the antibodies, was magnesium also present?

Rodkey: Yes, magnesium was present in the controls.

Gololobov: Magnesium is required for high activity. Without magnesium the rate is very low.

Green: There's no reaction without magnesium?

Rodkey: It's very, very low.

Green: Is there a reaction only with magnesium or without the antibody?

Rodkey: If you put in enough magnesium, yes. You can cleave DNA very efficiently with magnesium, but not at the low concentration used on our assays—about 1–10 m*M*.

Gololobov: The rates are corrected for the background incubation with magnesium.

Paul: A fundamental difference between induced fit by antibodies and transition-state binding antibodies can be expected in that the antibody specificity is directed at the unactivated ground state in the model that Scott and Gennady are proposing. On the other hand, conventional antibodies to transition-state analogs are meant to be specific for the transition state. My question is: Have you calculated the energetic equivalent of stretching the bond? How much free-energy contribution can you expect from the stress that is imposed on the bond?

Gololobov: We did not do a precise calculation, but I can quickly estimate that with a rate drop of 30 times, it is probably around 1–2 kcal per mol. That energy is basically delivered to the substrate by the antibodies in the form of the induced fit.

Paul: You pointed out this is mostly germline-encoded, right?

Scott: Yes, the residues that contribute to catalysis are encoded in the germline.

Kohler: Does that mean the immune system is trying to avoid this type of activity by not going through maturation and improving it?

Scott: I don't think that the immune system thinks this. One possibility is that catalysis was originally an important part of the germline function. As evolution improved upon antibody structure and started learning how to put in mutations, then some of the catalytic residues may have been thrown out, and we lost catalysis in favor of higher affinity. Several studies do suggest that in the germline there is a distinct possibility for a higher level of catalysis. But, of course, our transition-state intermediate experts argue that you need mutation to acquire catalytic potential. So it seems likely that we have the recognition of catalytic activity on both ends of this spectrum.

Kirby: This is a comment on the bond-lengthening question. The giveaway was the amount of energy he assumed was available to stretch the bond, and the energy was very small. To stretch a covalent bond takes an enormous amount of energy not available in a flexible protein network. When you change the conformation by the twisting proposed in your induced-fit mechanism, there will be a natural stereoelectronic effect on bond lengths that will mostly adjust back to normal bond lengths because of flexibility. This can change the reactivity to some extent—but a small extent.